Multi-point observations of the Hall electromagnetic field and secondary island formation during magnetic reconnection

J. P. Eastwood,[1] T.-D. Phan,[1] F. S. Mozer,[1] M. A. Shay,[2] M. Fujimoto,[3] A. Retinò,[4] M. Hesse,[5] A. Balogh,[6] E. A. Lucek,[6] and I. Dandouras[7]

Received 14 November 2006; revised 7 February 2007; accepted 22 February 2007; published 20 June 2007.

[1] A key feature of collisionless magnetic reconnection is the formation of Hall magnetic and electric field structure in the vicinity of the diffusion region. Here we present multi-point Cluster observations of a reconnection event in the near-Earth magnetotail where the diffusion region was nested by the Cluster spacecraft; we compare observations made simultaneously by different spacecraft on opposite sides of the magnetotail current sheet. This allows the spatial structure of both the electric and magnetic field to be probed. It is found that, close to the diffusion region, the magnetic field displays a symmetric quadrupole structure. The Hall electric field is symmetric, observed to be inwardly directed on both sides of the current sheet. It is large ($\sim$40 mV m^{-1}) on the earthward side of the diffusion region, but substantially weaker on the tailward side, suggesting a reduced reconnection rate reflected by a similar reduction in E_y. A small-scale magnetic flux rope was observed in conjunction with these observations. This flux rope, observed very close to the reconnection site and entrained in the plasma flow, may correspond to what have been termed secondary islands in computer simulations. The core magnetic field inside the flux rope is enhanced by a factor of 3, even though the lobe guide field is negligible. Observations of the electric field inside the magnetic island show extremely strong ($\sim$100 mV m^{-1}) fields which may play a significant role in the particle dynamics during reconnection.

Citation: Eastwood, J. P., T.-D. Phan, F. S. Mozer, M. A. Shay, M. Fujimoto, A. Retinò, M. Hesse, A. Balogh, E. A. Lucek, and I. Dandouras (2007), Multi-point observations of the Hall electromagnetic field and secondary island formation during magnetic reconnection, *J. Geophys. Res.*, *112*, A06235, doi:10.1029/2006JA012158.

1. Introduction

[2] Magnetic reconnection is thought to be one of the most fundamental processes controlling the dynamics of plasma. It is particularly important in the space environment, for example, controlling the interaction of the Earth's magnetosphere with the solar wind [*Dungey*, 1961]. Magnetic reconnection at the dayside magnetopause enables solar wind plasma to enter into the magnetosphere, resulting in the transient build up of magnetic flux inside the magnetosphere; magnetic reconnection in the magnetotail plays a key role in the dynamic changes that occur during the resulting magnetic storms and substorms.

[3] The first evidence supporting theories of reconnection was based on observations of macroscopic phenomena such as the existence of reconnection jets and, on a larger scale, the global behavior of the magnetosphere. However, this behavior is a consequence of reconnection, which does not strictly shed light on the specific causes of reconnection, of key importance when the plasma is collisionless. Theories of collisionless reconnection [*Vasyliunas*, 1975; *Sonnerup*, 1979] make specific predictions concerning the magnetic reconnection diffusion region. In particular, it is expected that the diffusion region exhibits a two-scale structure due to the differential motion of the electron and ion fluids. This leads to a characteristic Hall magnetic and electric field structure.

[4] The structure of the Hall fields, and particularly the Hall magnetic field, has been studied most extensively using simulations with symmetric inflow conditions. Recent work, for example, the GEM reconnection challenge [*Birn et al.*, 2001], predicts that the quadrupole Hall magnetic field is a distinctive feature of the diffusion region [e.g., *Hesse et al.*, 2001; *Pritchett*, 2001b; *Shay et al.*, 2001]. In the past few years a number of observations have been

[1]Space Sciences Laboratory, University of California, Berkeley, Berkeley, California, USA.
[2]Department of Physics and Astronomy, University of Delaware, Newark, Delaware, USA.
[3]Solar-Terrestrial Physics Group, Institute of Space and Astronautical Science, Sagamihara, Kanagawa, Japan.
[4]Swedish Institute of Space Physics, Uppsala, Sweden.
[5]Geospace Physics Branch, Laboratory for Solar and Space Physics, NASA Goddard Space Flight Center, Greenbelt, Maryland, USA.
[6]Space and Atmospheric Physics, The Blackett Laboratory, Imperial College London, London, UK.
[7]CESR-CNRS/UPS, Toulouse, France.

Copyright 2007 by the American Geophysical Union.
0148-0227/07/2006JA012158

reported confirming the existence of the Hall current loop [*Fujimoto et al.*, 1997] and the Hall magnetic field in the vicinity of the expected location of the reconnection site by the Geotail satellite in the near-Earth magnetotail [*Nagai et al.*, 2001; *Asano et al.*, 2004], by Wind in the distant magnetotail [*Øieroset et al.*, 2001], and by Polar at the dayside magnetopause [*Mozer et al.*, 2002]. More recently, the multispacecraft Cluster mission has also encountered Hall magnetic field signatures, both at the dayside magnetopause [*Vaivads et al.*, 2004] and in the near-Earth magnetotail [*Runov et al.*, 2003; *Borg et al.*, 2005; *Wygant et al.*, 2005; *Nakamura et al.*, 2006; *Xiao et al.*, 2006].

[5] The different behavior of the ions and electrons is also expected to result in Hall electric fields, as observed in simulations [*Shay et al.*, 1998; *Arzner and Scholer*, 2001; *Pritchett*, 2005a]. Hall electric field structure was first observed in Polar data [*Mozer et al.*, 2002], and subsequently in Cluster observations [*Vaivads et al.*, 2004; *Borg et al.*, 2005; *Wygant et al.*, 2005].

[6] The observations by Mozer et al. and Borg et al. are essentially single point in nature. Wygant et al. published comparisons between two Cluster spacecraft, which observed the same side of the diffusion region. In fact, Wygant et al. observed a bipolar structure in E_y^{GSE}, which was interpreted as a Hall electric field because of the twisting of the current sheet, placing the normal closer to the y_{GSE} direction rather than the usual z_{GSM}. In the event analyzed by Borg et al., they concluded that the GSM (geocentric solar magnetic) coordinate system was close to the current sheet system and that the normal was therefore closely aligned with the z_{GSM} direction. A second difference between the two events is that Wygant et al. observed the Hall electric field over a period of a few seconds, whereas Borg et al. observed it repeatedly over an interval of 4 min.

[7] Here we present new observations of what we have concluded to be a magnetic diffusion region in the near-Earth magnetotail. The observations are novel because different spacecraft observed the different quadrants of the Hall electromagnetic field structure at the same time, thus directly revealing the spatial structure. In particular, simultaneous observations of the electric field on both sides of the current sheet are presented for the first time.

[8] The observations were made by the Cluster spacecraft on 22 August 2001. We will focus on observations made between 09:40:00 and 09:52:00 UT, when the spacecraft encountered an earthward/tailward reversal in the plasma flow, correlated with a positive/negative reversal in the z_{GSM} component of the magnetic field. This particular magnetotail orbit has been studied by a number of researchers, each identifying and analyzing different features as follows: An earthward moving flux rope encountered at 10:08 UT by all four spacecraft was identified by *Slavin et al.* [2003b] who used the curlometer technique to investigate the nonforce-free nature of the flux rope. Subsequently, *Volwerk et al.* [2004] have studied part of the crossing (09:50–10:02 UT) in an analysis of compressional wave activity in high-speed flows. Observations from this current sheet crossing were also used in separate studies of magnetohydrodynamic eigenmodes in plasma sheet wave activity [*Fruit et al.*, 2004; *Louarn et al.*, 2004]. Finally, in an analysis of a later interval 09:50–09:58 UT, where the plasma velocity changed from tailward to earthward, *Lui et al.* [2006] have concluded that the observations during this later interval are inconsistent with magnetic reconnection but consistent with current disruption instead.

[9] The event studied here is of further interest because of the existence of an earthward-moving magnetic flux rope island and a tailward-moving island. Small-scale flux ropes ($\sim 10^0$ Earth radii in size) have been observed in the Earth's magnetotail using the ISEE spacecraft [*Elphic et al.*, 1986], Geotail [*Slavin et al.*, 2003a; *Ohtani et al.*, 2004], and Cluster [*Slavin et al.*, 2003b; *Eastwood et al.*, 2005, 2006]. One interpretation of these events is that reconnection occurs at several distinct sites [*Schindler*, 1974]. The reconnection rate at these sites may be different. In particular, if one site has evolved sufficiently such that it begins to process lobe plasma, the reconnection rate at that site is enhanced [*Hesse et al.*, 1996] and rapidly drives the other nascent flux rope structures earthward or tailward as appropriate [*Slavin et al.*, 2003a], although this may depend crucially on the stability of the ion tearing mode [*Sitnov et al.*, 2002].

[10] The formation of 'secondary' islands has been observed in several different simulations of magnetic reconnection [*Hesse et al.*, 1999; *Ohtani et al.*, 2004; *Drake et al.*, 2005; *Daughton et al.*, 2006]. It is thought that the guide field may play a key role in controlling the production and properties of such islands [*Drake et al.*, 2006b], but recent work using open boundary conditions suggests that islands will form even when no guide field is present [*Daughton et al.*, 2006]. Simulations also suggest that these structures play a key role in the production of energetic electrons [*Cattell et al.*, 2005; *Drake et al.*, 2006a] which is a problem of general importance in solar and cosmic plasma physics [*Lin et al.*, 2003].

[11] We have studied in detail the properties of the earthward-moving flux rope which exhibits particularly interesting electric field structure that, to our knowledge, has not been previously observed nor investigated by computational or theoretical means. We hope that such experimental information will spur the further development of simulations in a quest to understand the temporal evolution of the reconnection process.

[12] The remainder of this paper is organized as follows. In section 2, the data are described. In section 3, an overview of the observations is presented. In section 4, the Hall electric and magnetic signatures are analyzed in detail. In section 5, the structure of the secondary island is examined. The observations are discussed in the context of previously published theories, and our conclusions are presented, in section 6.

2. Data

[13] We present observations made by Cluster on 22 August 2001. During the time of interest, Cluster was located in the magnetotail plasma sheet, near the current sheet itself, approximately 19 R_e from the Earth. The Cluster mission consists of four identical spacecraft in polar orbits around the Earth [*Escoubet et al.*, 2001]. In this part of the mission, the orbits were arranged so that the spacecraft formed a tetrahedron during apogee with a scale size of $\sim$2000 km. For a plasma density of 0.1 cm^{-3}, this

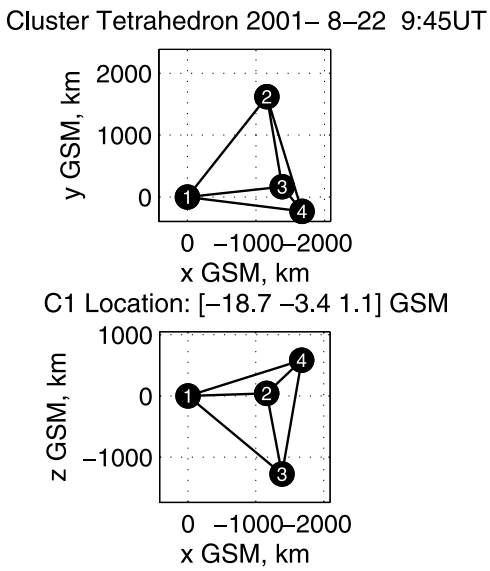

Figure 1. Configuration of the Cluster tetrahedron on 22 August 2001, at 09:45 UT. The positions of the spacecraft are shown relative to Cluster 1, in the geocentric solar magnetic coordinate system. The scale size of the tetrahedron was ~2000 km.

corresponds to ~3 ion inertial lengths (c/ω_{pi} = 720 km). Figure 1 shows the configuration of the Cluster tetrahedron at 09:45 UT on 22 August 2001. The top panel shows the tetrahedron projected into the *x*-*y* geocentric solar magnetic (GSM) coordinate system; the bottom panel shows the projection into the *x*-*z* GSM plane. Note that the *x* axis is directed so that the Earth is to the left. The positions of the spacecraft are shown in kilometers relative to Cluster 1. Cluster 1 is located at (−18.7, −3.4, 1.1) R_e (GSM). Cluster 1, 2, and 4 form a plane that is nearly parallel to the *x*-*y* plane. Cluster 3 lies below this plane. Finally, Cluster 1 is closest to the Earth.

[14] The analysis has used data from several different instruments. Magnetic field observations are taken from the FGM instrument [*Balogh et al.*, 2001], which measures the three components of the DC magnetic field. The data are available at 22.42 vectors/s, which is the resolution used in this work unless otherwise stated. Electric field observations are taken from the EFW instrument [*Gustafsson et al.*, 2001], which uses four sensors at the end of wire booms to measure the components of the DC electric field in the spin plane of the spacecraft [the spin plane is nearly parallel to the geocentric solar ecliptic (GSE) *x*-*y* plane]. The data are available at a resolution of 25 vectors/s. The third component of the electric field (along the spin axis) can be reconstructed using the magnetic field if it is assumed that $\mathbf{E} \cdot \mathbf{B} = 0$, i.e., that there is no parallel electric field. This assumption is expected to be valid everywhere except in the electron diffusion region itself. In this case, equation (1) is used to calculate the spin axis component

$$E_z = -\left(\frac{B_x}{B_z}\right)E_x - \left(\frac{B_y}{B_z}\right)E_y \qquad (1)$$

where the subscripts *x* and *y* refer to the spin plane components and *z* the spin axis component. Clearly, if (B_x/B_z) is large, small errors in E_x will be amplified resulting in errors in E_z. Also, if B_z is close to zero, the same problem will manifest itself. Consequently, the reconstruction of the electric field is only possible when (1) the magnetic field is not too weak and (2) the magnetic field is not close to the spin plane. Typical threshold values for reconstruction, on the basis of prior experience, are $|B_z| > 2$ nT, $|B_x/B_z| < 10$.

[15] Observations of the ion plasma are taken from the CIS instrument [*Rème et al.*, 2001]. CIS consists of the following two detectors: HIA, which measures the ion population without mass discrimination, and CODIF, which includes a time of flight section. Data are not available from the CIS instrument on spacecraft 2, and CIS-HIA data are not available on spacecraft 4. The detectors measure the ion population up to an energy of ~40 keV. Moments of the distribution are computed on board at 4-s (spin) resolution. Full three-dimensional distributions are produced at 12-s resolution. In this analysis, data from HIA has been used unless otherwise stated.

3. Overview

[16] Figure 2 shows an overview of the observations from Cluster between 09:40:00 and 09:52:00UT on 22 August 2001 (day 234). The magnetic and electric fields from all four spacecraft are shown at 4-s (spin) resolution, together with the plasma data from Cluster 1 and Cluster 3. The top panel shows the differential energy flux as measured by Cluster 3. Note that the data are shown in the GSM coordinate system and that the spin axis electric field has been reconstructed under the assumption that $\mathbf{E} \cdot \mathbf{B} = 0$, subject to the caveats described in the previous section. All four spacecraft are initially located above the current sheet ($B_x > 0$), and during the interval they cross the current sheet. They do not cross simultaneously, and there is significant decorrelation between the spacecraft time series; the spacecraft separation is somewhat larger than the scale thickness of the current sheet. Also, note that the magnetic field above the current sheet (close to the lobe) does not contain a significant guide field (cf. Figure 2 at 09:40 UT).

[17] This interval was identified because of the correlated reversal in the *x* component of the plasma velocity and the *z* component of the magnetic field. At 09:44:25 UT, the Cluster spacecraft observed a correlated positive/negative reversal; this signature is usually interpreted as an *X* line [*Ueno et al.*, 1999], which given the positive/negative reversal is moving earthward relative to the spacecraft. Initially, the earthward flow is ~750 km s^{-1} and reverses to a weaker flow of ~200 km s^{-1}. This event is marked by the vertical black line in Figure 2. At 09:50 UT, a stronger tailward flow is observed, exceeding 800 km s^{-1} in the antisunward direction at Cluster 1. Finally, we note the existence of significant v_y ion plasma flows in the vicinity of the reconnection region. These flows have not been widely reported in experimental data, but are qualitatively consistent with results from some simulation studies [*Shay et al.*, 2004]. In the ion diffusion region, the ions are directly accelerated in the out-of-plane direction by the reconnection electric field, as observed in simulations [*Pritchett*, 2001a].

[18] A key question, motivated by our previous work, is whether the timing of events at the different spacecraft is consistent with this *X*-type geometry. In the analysis of a

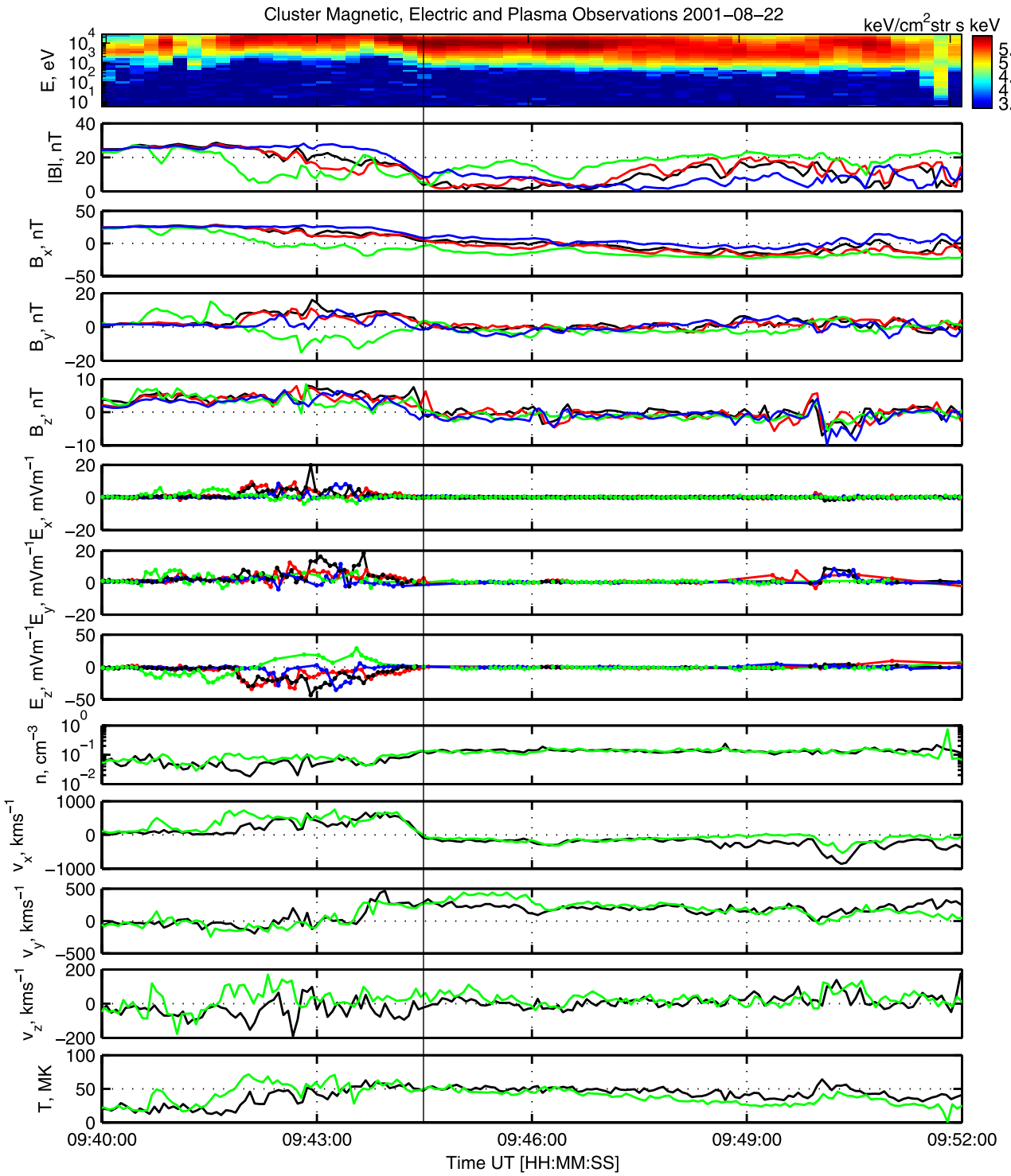

Figure 2. Overview of the electric field, magnetic field, and ion plasma observed by Cluster between 09:40:00 and 09:52:00 UT on 22 August 2001. The top panel shows the differential energy flux measured by Cluster 3. The next four panels show the magnetic field magnitude and the components of the magnetic field in the GSM coordinate system. Vector data are shown at 4-s resolution and black, red, green, and blue are used to denote Cluster 1 to Cluster 4. The next three panels show the electric field data. The spin axis electric field has been reconstructed under the assumption that $\mathbf{E} \cdot \mathbf{B} = 0$. The next five panels show the ion plasma density, velocity, and temperature. Only data from Cluster 1 and Cluster 3 is shown.

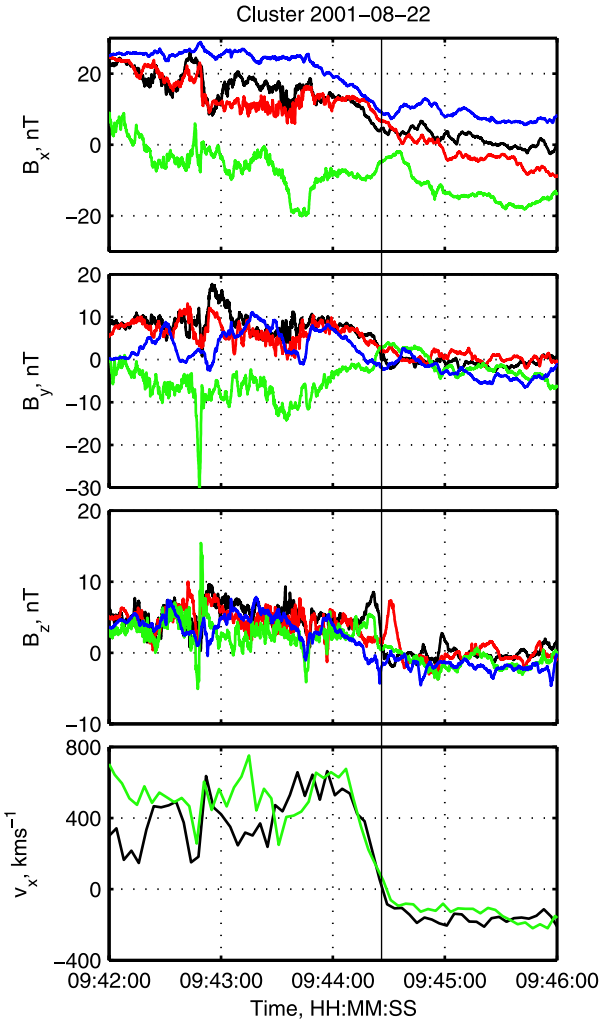

Figure 3. Magnetic field observed by all four spacecraft between 09:42:00 and 09:46:00 UT. The data are shown in the GSM coordinate system at high resolution. The bottom panel shows the x component of the plasma velocity. The vertical black line marks the reversal in flow.

somewhat similar correlated field and flow reversal, observed on 2 October 2003, it was found that this signal is not a unique identifier of an X line [*Eastwood et al.*, 2005]. In fact, by using a multispacecraft analysis, it was found that the signature corresponded to a magnetic island, or flux rope, bound by two distinct X lines. Only a multispacecraft analysis allows the true structure of the event to be established. In the 2 October 2003 event, the spacecraft separation was only 300 km and the magnetic field time series were extremely well correlated. This allowed a quantitative approach using a timing analysis [*Schwartz*, 1998]. Here the separation is approximately one order of magnitude larger, and the time series are not sufficiently well correlated to perform a quantitative four-point timing analysis. Nevertheless, a qualitative judgment can be reached and limited quantitative estimates can be made.

[19] Figure 3 shows the magnetic field observed by all four spacecraft in the vicinity of the magnetic field reversal. During the interval shown, all the spacecraft are in the process of crossing the current sheet (because of relative motion between the current sheet and the spacecraft in the z direction) and the spacecraft are located at different points in the current sheet, on the basis of the observed values of B_x. Referring to the measurements of B_z, Cluster 1 observes the reversal in B_z after Cluster 3, indicating earthward motion of this feature. This can also be seen in Figure 4. Cluster 2, which is dawnward of the other spacecraft, is the last to observe the reversal, suggesting some structuring in the y direction. Unfortunately, it was not possible to make any estimate of the lateral motion of the X line. Analysis of similar encounters at smaller separations may enable such an analysis. However, we may conclude that the structure is moving toward the Earth and that this is thus most likely an X-type configuration. This may account for some of the difference in the magnitude of the tailward and earthward flows. If an X line is generating equal tailward and earthward flow, an observer moving relative to the X line would observe unequal flows. If the X line is relatively moving earthward, this may mean that the earthward flow is larger. Alternatively, this may be due to a reduction in the reconnection rate that occurred close to the time of observation. This is discussed in more detail below where the electric field observations are analyzed.

[20] At the start of the interval shown in Figure 3, all of the spacecraft observe positive B_x and are thus above the current sheet. At 09:42:19 UT, Cluster 3 crossed the current sheet and observed a negative B_x for the remainder of the interval. At the time of the reversal in B_z (just after

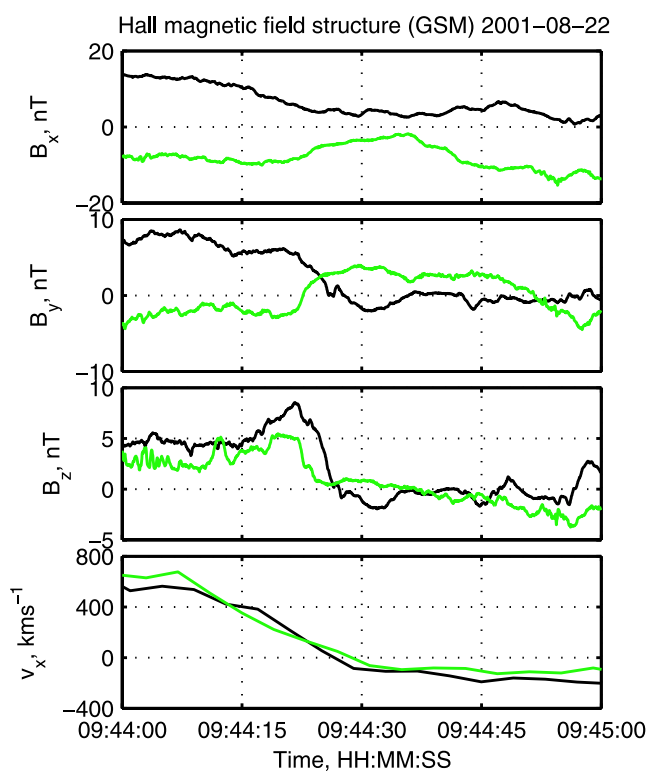

Figure 4. Dual spacecraft observations of the Hall magnetic field structure. Cluster 1 (black), which passes above the diffusion region, observes a positive/negative transition in B_y. Cluster 3 (green), which passes below the diffusion region, observes the mirror image profile in B_y. This is illustrated in more detail in Figure 12.

Table 1. Results of Minimum Variance Analysis Applied to Cluster 3 Magnetic Field Data Between 09:40:00 and 09:45:00 UT

	Eigenvalue	Eigenvector
Minimum	4	(0.12, −0.08, −0.99)
Intermediate	21	(0.34, −0.93, 0.12)
Maximum	224	(0.93, 0.35, 0.08)

09:44:00 UT and marked by the vertical black line), Cluster 3 was below the current sheet with the other spacecraft remaining above the current sheet.

[21] Finally, we describe observations of two bipolar structures in the B_z time series. At 09:50 UT, the tailward flow speed increases, exceeding 800 km s^{-1} in the tailward direction at Cluster 1. Embedded in the leading edge of this flow is a bipolar positive-negative perturbation in B_z, which is consistent with a magnetic island structure moving tailward [*Slavin et al.*, 2003a]. This structure is observed by all four spacecraft, and it is thus possible to determine its motion from the multispacecraft observations. It is found that the structure is moving tailward at a speed of ~600 km s^{-1}, which is comparable with the observed flow velocity thus implying that the structure is convected in the reconnection outflow.

[22] The second was observed by Cluster 3 (green) at 09:42:49 UT (Figure 3). This negative/positive signature in B_z, accompanied by a spike in the core B_y field, corresponds to an earthward-moving magnetic flux rope/island and is discussed in more detail in section 5.

[23] Before examining the observations in more detail, we discuss our choice of coordinate systems. Because the spacecraft separation is large relative to the structures of interest, the individual spacecraft time series are not well correlated and one cannot use multispacecraft methods to quantitatively determine, for example, the current sheet normal [*Dunlop et al.*, 1988]. However, minimum variance analysis (MVA) can be used to determine the current sheet orientation; if the minimum variance direction is well defined, then it is identified as the current sheet normal [*Sonnerup and Scheible*, 1998]. MVA should not be applied to the whole data interval shown in Figure 2, since B_z reverses in addition to B_x for all the spacecraft, and thus the assumption that the normal (~z component) of the field is constant is invalid. However, it can be applied to the reversal in B_x observed by Cluster 3 at 09:42:18 UT. Applying MVA to the interval 09:40:00 to 09:45:00 UT, a minimum variance direction of (0.11, −0.08, −0.99) is obtained. The ratio of intermediate to minimum eigenvalues is 5.2. The full results of the MVA analysis are shown in Table 1. The MVA estimate of the current sheet normal is within ~8° of the z_{GSM} direction. The intermediate and maximum variance directions are rotated by ~20° relative to the x_{GSM} and y_{GSM} directions. Since the current sheet tilt is small, we have chosen to describe the data by simply using the GSM coordinate system. This avoids any problems that may arise due to the remaining uncertainties in the determination of the minimum variance direction, for example, the variation of the normal with specific interval chosen. As is shown in the next section, the Hall electric and magnetic field structure is evident in GSM without further processing of the data. Finally, we note that the rotation angle between the GSM and GSE coordinate systems is ~30°. This is significant and implies that GSE is not an appropriate coordinate system to use when analyzing the data.

4. Hall Magnetic and Electric Field Signatures

[24] We now examine the region around the flow reversal in more detail. Figure 4 shows the three components of the magnetic field observed by Cluster 1 and Cluster 3 between 09:44:00 and 09:45:00 UT, together with the x component of the plasma velocity. Cluster 1 observes positive B_x and is one of the three spacecraft above the current sheet. Cluster 3 was below the current sheet, indicated by negative B_x. Cluster 3 encounters the reversal in B_z first, which is consistent with an overall earthward motion of the diffusion region as discussed in the previous section. The second panel shows the B_y component, where one expects to observe Hall magnetic field effects, should they be present. The spacecraft observed opposite reversals in B_y. Cluster 1, above the current sheet, observed a positive/negative reversal, whereas Cluster 3, below the current sheet, observed a negative/positive reversal. To illustrate this in more detail, Figure 5 shows B_x plotted as a function of v_x for Cluster 1 and Cluster 3 between 09:43:00 and 09:45:00 UT (HIA was only operating on these spacecraft). The data are plotted as open circles, with the radius of the circle corresponding to the magnitude of B_y and the color corresponding to its sign. Black indicates that B_y is positive, and red indicates that B_y is negative. The overall quadrupole pattern derived from data from the two spacecraft is consistent with the expected Hall magnetic field signature. There are some points in the bottom left quadrant which are red instead of black, indicating negative values of B_y which are inconsistent with the Hall magnetic field. However, the magnitude of the inconsistent data points is small. A further inspection of

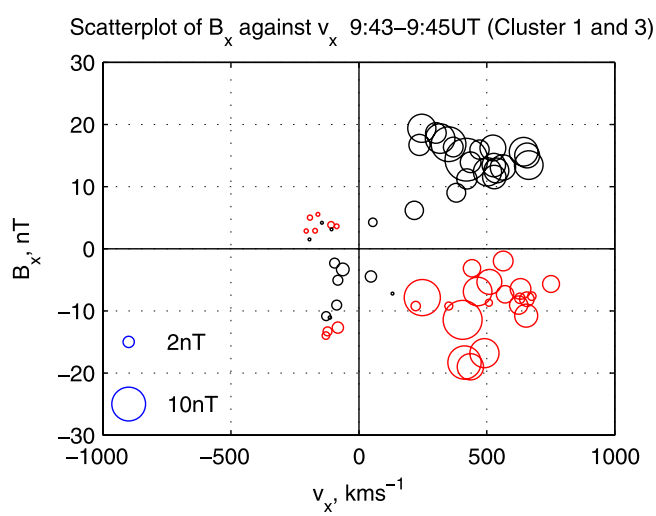

Figure 5. Scatterplot of v_x and B_x observations made by Cluster 1 and Cluster 3 between 09:43:00 and 09:45:00 UT on 22 August 2001. The color of the circles show the sign of B_y. Black corresponds to positive B_y and red to negative B_y. The size of the circle shows the magnitude of B_y (the blue circles in the bottom left corner show the corresponding scale and are not data points).

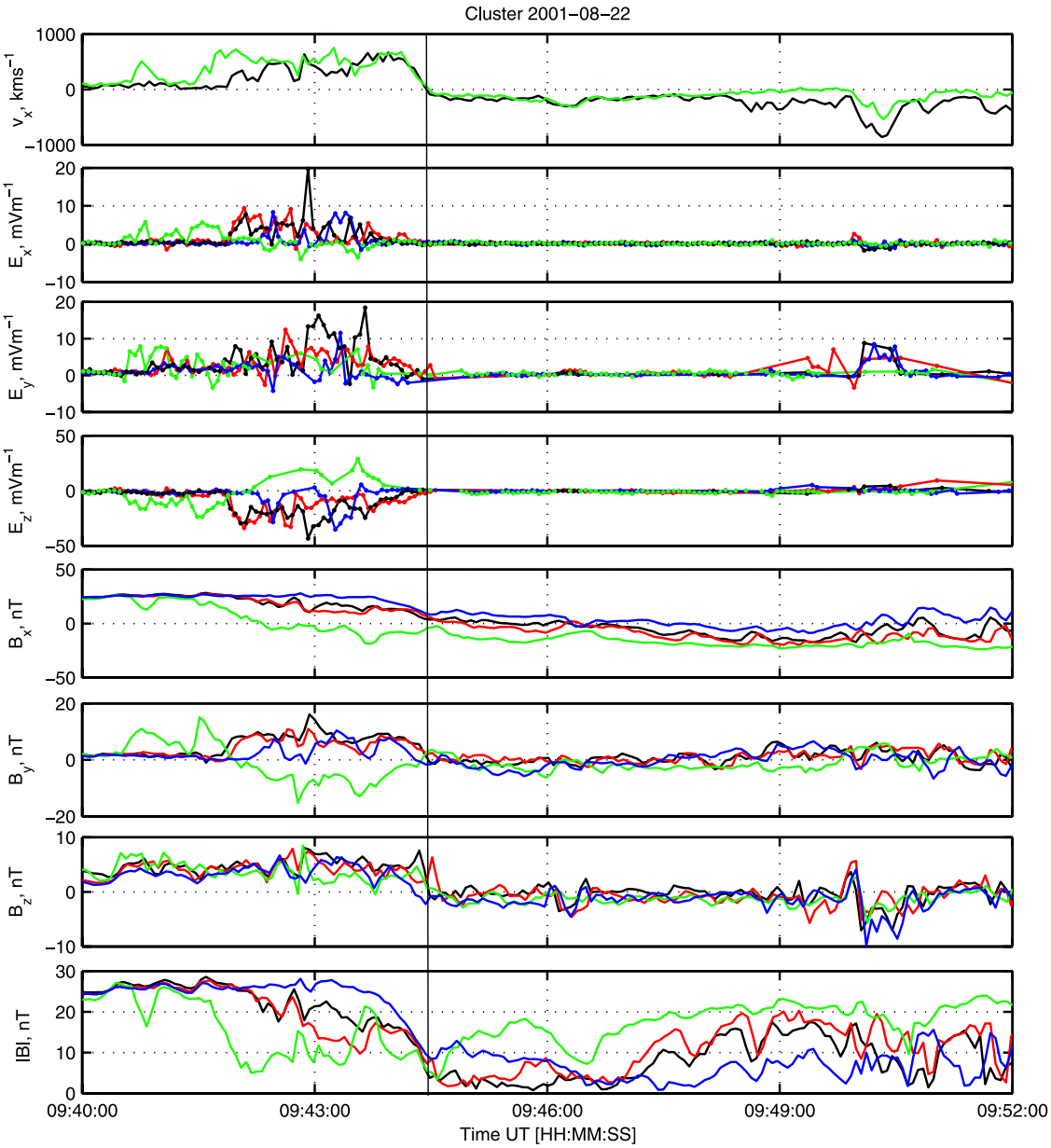

Figure 6. Electric and magnetic fields observed by all four spacecraft between 09:40 and 09:52 UT.

the data shows that these data were recorded by Cluster 3 at the end of the interval, and thus at the edge of this region. This is discussed in more detail later in this section.

[25] We now consider the electric field observations, in particular, the E_z component where theory predicts the Hall electric field to be observed [e.g., *Shay et al.*, 1998; *Pritchett*, 2005b]. Figure 6 shows the electric and magnetic field observed by all four spacecraft between 09:40 and 09:52 UT. Initially, all spacecraft were located in the northern lobe and observed a quiet electric field. At 09:40:37 UT, Cluster 3 observed strong negative E_z coinciding with its transit into the plasma sheet proper and the first observations of the earthward flow. A negative E_z of, on average, approximately −15 mV/m but reaching as low as −35 mV/m was recorded. It also observed a strong Hall magnetic field in the B_y component. At 09:41:49 UT, Cluster 1 and Cluster 2 transited into the plasma sheet and encountered similar negative E_z. Shortly afterward, at 09:42:10 UT, Cluster 3 crossed the current sheet and simultaneously observed a reversal in E_z from negative to positive values. As this occurred, Cluster 4 finally entered the plasma sheet on the north side, observing negative E_z. For more than 1 min prior to the reversal in B_z (at 09:44:25, marked by the black vertical line), Cluster 1, Cluster 2, and Cluster 4 observed negative E_z above the current sheet while, simultaneously, Cluster 3, below the current sheet, observed positive E_z. That is, the electric field was observed to point into the current sheet on both sides.

[26] The source of the measured electric field is described by the generalized Ohm's law

$$\mathbf{E} = -\mathbf{v}_\mathbf{i} \times \mathbf{B} + \frac{1}{\mathrm{ne}}\mathbf{j} \times \mathbf{B} - \frac{1}{\mathrm{ne}}\nabla \cdot \mathbf{P}_\mathbf{e} - \frac{m_e}{e}\frac{\mathrm{d}\mathbf{v}_\mathbf{e}}{\mathrm{d}t} + \eta \mathbf{j} \qquad (2)$$

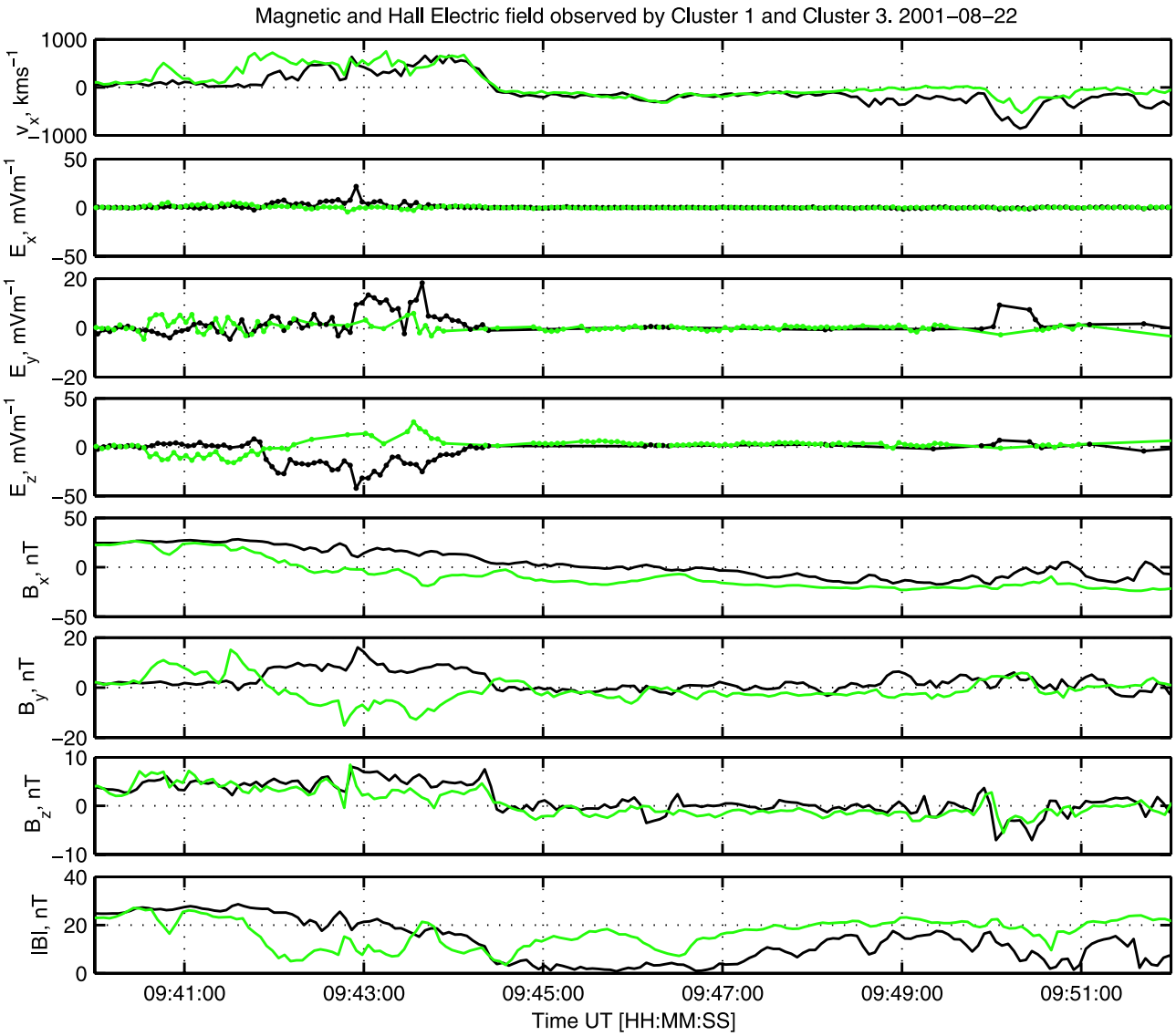

Figure 7. The Hall electric field and the magnetic field as observed by Cluster 1 and Cluster 3 between 09:40 and 09:52 UT on 22 August 2001. The plotted electric field is $\mathbf{E} + \mathbf{v_i} \times \mathbf{B}$.

In most regions of geospace, only the first term on the right-hand side of equation (2) is considered important. However, in the vicinity of reconnection sites, the other terms are nonnegligible. In these observations, we note that ion plasma flow has a strong v_y component, particularly between 09:44 and 09:50 UT. This flow may represent part of the reconnection jet or a lateral motion of the magnetotail plasma relative to the spacecraft. However, in order to determine the Hall component of the electric field, we have computed $\mathbf{E} + \mathbf{v_i} \times \mathbf{B}$ at Cluster 1 and Cluster 3, where velocity data are available. The resulting electric field, which is likely to be dominated by the $\mathbf{j} \times \mathbf{B}$ term in equation (2), the Hall field, is plotted in Figure 7. Cluster 3 is in the southern hemisphere and observes a positive Hall field on the tailward side of the X line. Cluster 1 resides close to the current sheet after the passage of the X line and observes a negligible Hall field.

[27] Figure 8 shows a scatterplot of the Hall E_z (panel 4 of Figure 7) as a function of B_x (panel 5 of Figure 7) between 09:43:00 and 09:45:00 UT (the same interval as Figure 5). Data from Cluster 1 and Cluster 3 are shown; points are colored according to the spacecraft. Cluster 1, above the current sheet, observed negative values of E_z, reaching approximately -30 mV m^{-1}. Cluster 3, simultaneously below the current sheet, observed positive values of E_z, of similar magnitude. By combining the observations, the electric field structure is seen to be consistent with the expected Hall field. To our knowledge, this is the first time that such simultaneous observations from both sides of the current sheet have been reported. Figure 8 also shows that the Hall field is minimized at the center of the current sheet itself. This is consistent with previous observations [*Borg et al.*, 2005].

[28] At 09:44:25 UT, Cluster passed from the earthward to the tailward side of the diffusion region. A significant weakening of the electric field was observed. For example, the electric field component E_z at Cluster 3 was observed to be $\sim$5 mV m^{-1} at 09:44:53 UT after the reversal. After the

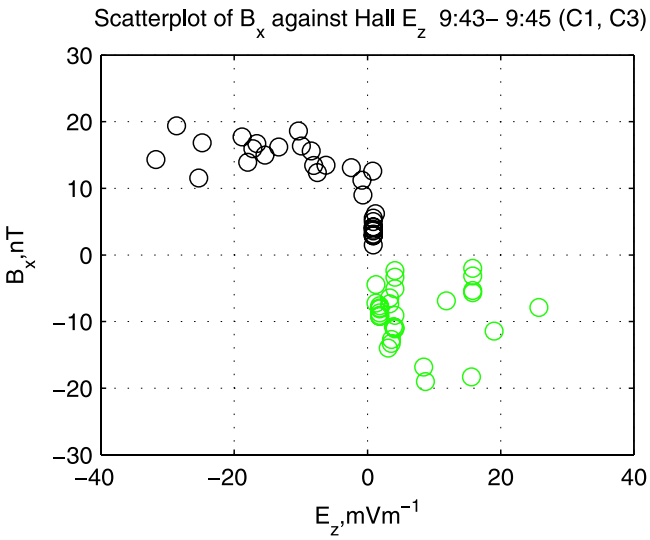

Figure 8. Scatterplot showing B_x as a function of the z component of the Hall electric field during the interval 09:43:00–09:45:00 UT, as observed by Cluster 1 (black) and Cluster 3 (green).

crossing, the magnetic field observed by Cluster 1 especially is very weak, consistent with the spacecraft being close to the current sheet, as also indicated by the small value of B_x. This made it difficult to reconstruct the electric field at this spacecraft. At 09:50:00 UT, when a strong tailward burst was observed, Cluster 3 observed $E_z \sim 10$ mV m^{-1}.

[29] The asymmetry between the tailward and earthward observations may be due to temporal variations in the reconnection rate. Figure 9 shows a scatterplot of E_y as a function of B_x during the interval containing the flow reversal and using data from all four spacecraft. E_y is measured in the spacecraft frame. The figure shows that the cross-tail electric field (E_y) is predominantly positive during this event, consistent with reconnection. The average value of E_y in the interval preceding the flow reversal was 3.1 mV m^{-1}. The average of E_y in the interval following the flow reversal was 0.3 mV m^{-1}. The largest individual observations of E_y were seen during the earthward flow, reaching values of up to $\sim$20 mV m^{-1}.

[30] However, it is important to remember that the observations are presented in the spacecraft frame, not the rest frame of the X line. In particular, if the X line is moving earthward with a velocity u, it can be shown that the electric field E_y is enhanced on the earthward side and reduced on the tailward side. For example, if $u = 100$ km s^{-1}, and $B_z = 5$ nT, E_y is increased (reduced) by 0.5 mV m^{-1} on the earthward (tailward) side of the X line. However, this effect cannot explain the reduction in the magnitude of the Hall fields. Therefore, although some of the observed asymmetry can be explained by the relative earthward motion of the X line, there may also be a temporal reduction in the reconnection rate.

[31] We now consider on a more quantitative basis the results shown here in the context of previous observations and simulations. Simulations [*Shay et al.*, 1998; *Birn et al.*, 2001] suggest that the out-of-plane magnetic field can attain a significant (20–40%) fraction of the lobe magnetic field strength B_0 [*Hesse et al.*, 2001]. In the example presented here, the lobe magnetic field strength is of the order of 30–40 nT, suggesting that Hall fields of 10–16 nT should not be unexpected, particularly away from the midplane of the current sheet. Referring to Figure 5, the largest absolute value of B_y was 14.2 nT, observed by Cluster 1.

[32] To determine the expected value of the Hall electric field, we may treat the plasma as a single fluid subject to the Generalized Ohm's law. Neglecting all terms except for the Hall term, we find

$$\mathbf{E} = \frac{\mathbf{j} \times \mathbf{B}}{\mathrm{ne}} \tag{3}$$

[33] If it is assumed that the current is carried by the electrons, this equation reduces to the electron momentum equation in the two fluid model.

$$E_z = v_{e,y} B_x \tag{4}$$

[34] There exist techniques which can be used, in certain specific circumstances, to estimate E_{hall} from the multi-point magnetic field data directly; For example, the curlometer technique [*Dunlop et al.*, 2002] can be used to determine the current density, which can then be used to find $\mathbf{j} \times \mathbf{B}$. The technique assumes that the magnetic field varies linearly between the spacecraft and should only be applied when the tetrahedron is significantly smaller than the current sheet thickness (for example the heliospheric current sheet [*Eastwood et al.*, 2002]). However, $\mathbf{j}$ cannot be computed reliably here because the spacecraft separation is comparable to the structure of interest (the current sheet) and the magnetic field does not vary linearly between the spacecraft. Furthermore, in computing $\mathbf{j} \times \mathbf{B}$, $\mathbf{j}$ is constant over the tetrahedron, and so $\mathbf{j} \times \mathbf{B}$ is different at each spacecraft. If the magnetic

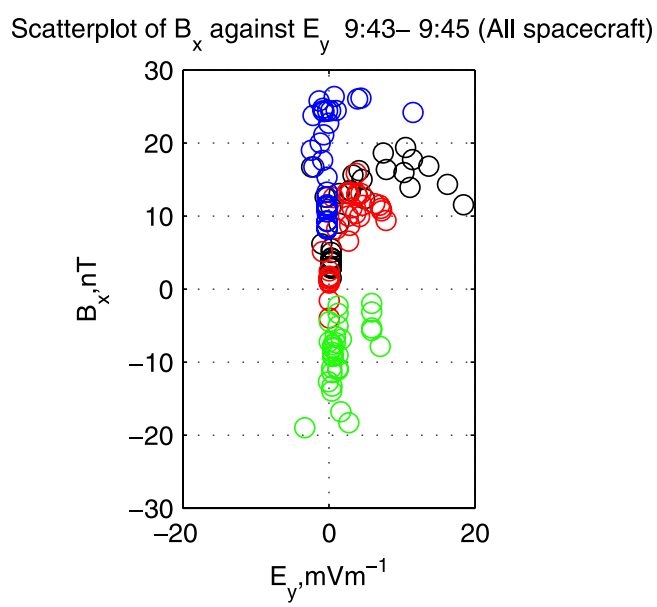

Figure 9. Scatterplot of B_x as a function of E_y between 09:43:00 and 09:45:00 UT, using data from all four spacecraft. Note that E_y is, on average, greater than zero, as expected during reconnection events.

field observed at each spacecraft has a similar orientation, this may not be too difficult a problem to overcome. However, if the spacecraft straddle the current sheet, it is (1) unclear how **B** should be averaged (if at all) and (2) likely that the curlometer estimate of **j** is unreliable.

[35] If the orientation and normal speed of the current sheet is known, then under the assumptions of stationarity and one-dimensional structure, the current density could be estimated by differentiating the magnetic field time series [*Vaivads et al.*, 2004]. However, here the normal speed of the current sheet relative to the spacecraft is unknown. This motion ought to be reflected in slightly different values of E_y on either side of the current sheet. However, a speed of 10 km s^{-1}, for example, corresponds to an electric field offset of 0.1 mV m^{-1} in a 10 nT magnetic field, which is unobservable in this event.

[36] In simulations, the magnetic field is typically normalized to the lobe magnetic field strength and the velocities to an Alfven speed based on the lobe field and the plasma sheet density. In simulations, a Hall electric field of up to 0.5 in normalized units has been reported [*Shay et al.*, 1998]. If the lobe field strength is 20 nT and the plasma sheet density is 0.1 cm^{-3}, this corresponds to a measured electric field of 10 mV m^{-1}. A lobe field of 40 nT corresponds to a measured electric field of ~50 mV m^{-1}. The largest observed absolute value of E_z was approximately 35 mV m^{-1}, which indicates that the simulations are in relatively good agreement with the observations.

5. Properties of an Associated Magnetic Island

[37] As mentioned in section 3, a small-scale magnetic flux rope was observed during this event. Figure 10 shows the magnetic field observed by each of the four spacecraft between 09:42:30 and 09:43:00 UT, a period of 30 s. Cluster 3, which was close to the current sheet (on the basis of the small value of B_x) observed a strong bipolar signature in B_z at 09:42:48 UT. This was accompanied by a spike in the magnitude of the B_y component and an increase in the field strength. This time series profile, when embedded in earthward plasma flow, is conventionally interpreted as an Earthward-moving flux rope structure [*Elphic et al.*, 1986; *Slavin et al.*, 2003a; *Henderson et al.*, 2006].

[38] The fact that the structure was only observed by one spacecraft (Cluster 3) precludes the use of multi-point analysis. However, this can be used to set an upper limit on the structure diameter perpendicular to the flow. Cluster 3 was close to the current sheet midplane, but on the opposite side to the other spacecraft. If we assume the axis of the flux rope to be close to the current sheet plane and Cluster 3, then since the separation between Cluster 1 and Cluster 3 in the z direction is ~1300 km, a maximum transverse diameter of ~2600 km is implied. The magnetic field observed at Cluster 4 particularly is characteristic of a Traveling Compression Region [*Slavin et al.*, 2005].

[39] The flux rope passes over the spacecraft in a period of approximately 5 s. The ion plasma flow speed is ~500 km s^{-1}, which corresponds to a diameter of ~2500 km. However, these observations are made in the vicinity of the ion diffusion region. This means that the electron plasma (to which the magnetic field is frozen) may be moving differentially to the ion plasma. An alternative approach is to calculate the velocity $\mathbf{v} = (\mathbf{E} \times \mathbf{B})/B^2$. We therefore now consider the available electric field data.

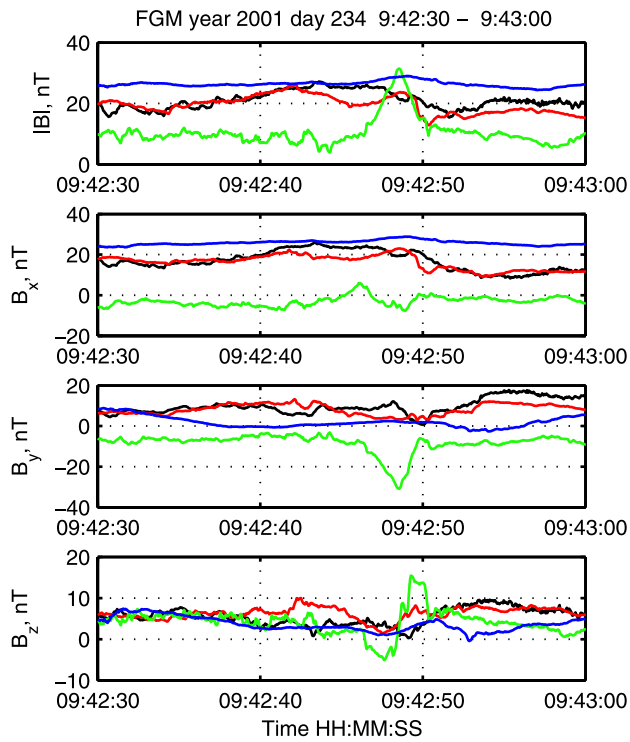

Figure 10. Secondary island observed by Cluster 3 in the outflow region of the X line. The top panel shows the magnetic field strength, and the other three panels show the B_x, B_y, and B_z components of the magnetic field in GSM.

[40] The electric field signature of the secondary island, in the spacecraft frame, is shown in Figure 11. Only 6 s of data are shown. Several features are immediately apparent. There is a negative/positive/negative tripolar signature in the x component of the electric field. The peak-to-peak amplitude is ~100 mV m^{-1}. Second, E_y is seen to become more negative at 09:42:48 UT, rapidly reversing sign at 09:42:48.5 UT, and then remaining positive. This reversal in E_y occurs at the same time as the reversal in B_z. Finally, in the center of the flux rope, a positive E_z of greater than 100 mV m^{-1}, peaking at nearly 150 mV m^{-1} is observed. Note that the E_z outside the structure is also positive, but is dwarfed by the field inside the flux rope. These large fields are observed for about 1 s at the core of the magnetic field flux rope where B_y is maximized. By comparison, during the passage of the tailward-moving island at 09:50 UT, no enhancement of the core field, or the electric field, is observed.

[41] The magnetic field strength in the center of the secondary island is ~32 nT, compared with ~10 nT just outside. This factor of 3 increase is almost entirely due to the increase in $|B_y|$ from 8 to 31 nT. Almost simultaneously, E_z peaks at ~150 mV m^{-1}. If we neglect the other components of **E**, and if $|B|$ = 32 nT and $B_x = -10$ nT, we find that $v_y = B_x E_z/|B|^2 \sim -1000$ km s^{-1} and $v_x = -B_y E_z/|B|^2 \sim 3000$ km s^{-1}. This is approximately 10% of the local electron Alfven speed. If the ion inertial length is ~10^3 km (if n = 0.1 cm^{-3}, c/ω_{pi} = 720 km), we can conclude that the island length is probably of the order of

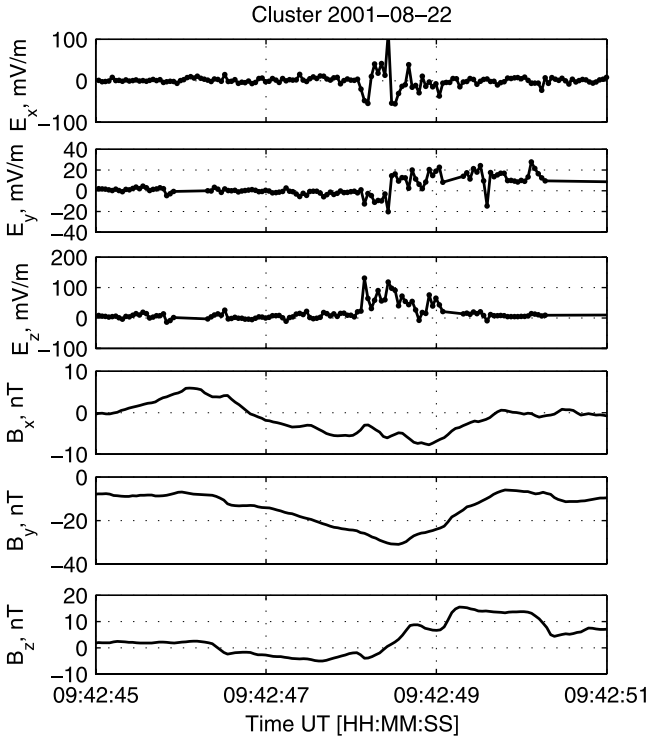

Figure 11. Electric field structure inside the secondary island observed by Cluster 3 at 09:42:48 UT.

10–20 c/ω_{pi}. The electric field is then structured on scales comparable to c/ω_{pi}. Unfortunately, there are technical problems with the electron observations from spacecraft 3, and so it is not possible to compare the $\mathbf{E} \times \mathbf{B}$ and electron velocities.

[42] We may further estimate the current that the out-of-plane velocity corresponds to. Given $v_{e,y} = 10^3$ km s^{-1}, and assuming that the current is carried entirely by the electron population with density 0.1 cm^{-3}, we find that $j_y = n_e e v_{e,y} = -16$ nA m^{-2}. The change in B_x is of the order of 30 nT (comparing different spacecraft observations). Using Ampere's law, this gives an estimated length scale of 10^3 km, which is of the order of an ion inertial length, less than the spacecraft separation and consistent with the observations.

[43] It would appear that a significant component of the ambient magnetic field is due to the Hall magnetic field. In simulations, the enhancement of the core field is driven by compression of the guide field, because secondary islands are observed at the current sheet itself, where the Hall magnetic field is zero. These results suggest that, even if the overall guide field is small, secondary islands with extremely large core fields can arise, if the island is produced in a region with a locally large B_y, such as generated by Hall effects. However, for this to be true, it would seem that the magnetic island must be formed away from the current sheet plane, since $B_y = 0$ at the current sheet itself; how this occurs exactly is a challenge for simulations.

6. Summary and Conclusions

[44] In this paper, we have presented new Cluster observations of what has been interpreted as a magnetic reconnection site in the near-Earth magnetotail. The multi-point observations of Cluster have been used to examine the spatial structure of the Hall magnetic and electric fields surrounding the diffusion region. We have also presented observations of a secondary island, which exhibited an extremely large core field, despite the lack of an overall guide field, and large internal electric fields. This earthward-moving flux rope, with a strong guide field and strong electric fields, may be compared to the tailward-moving island that is also observed. The tailward moving structure, which is larger, does not exhibit either an enhancement in the guide field or strong electric fields. Once the reconnection site was earthward of the spacecraft, this structure developed and was ejected, convected in the tailward-moving flow and overtaking the spacecraft. Such island ejection has been observed in simulations [e.g., *Drake et al.*, 2006a].

[45] In Figure 12, a cartoon is used to qualitatively interpret the observations made by Cluster 1 and Cluster 3. While this picture provides a conceptual basis for understanding the data, it should be used with care. In particular, it does not accurately reflect the temporal changes that occurred during the event (particularly the reduction in the reconnection rate that occurred almost simultaneously with the passage of the spacecraft from the earthward to the tailward outflow region and the tailward island ejection). We only show the history of Cluster 1 and Cluster 3, since these spacecraft made the most complete observations. Furthermore, the presence of the v_y ion plasma flow must be borne in mind. The existence of such

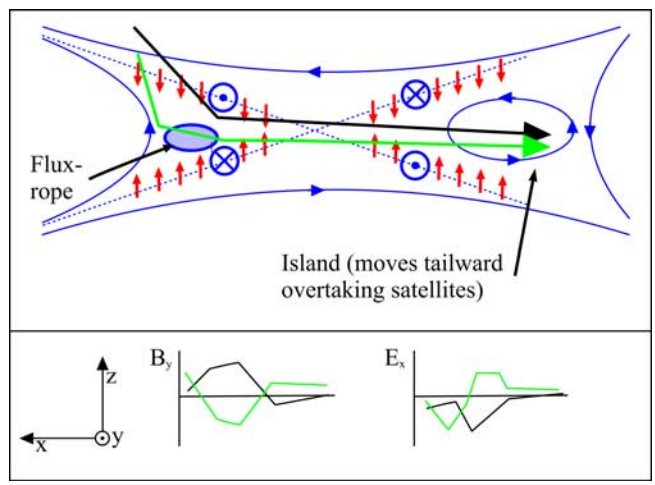

Figure 12. Cartoon interpreting the electric and magnetic fields observed by Cluster 1 and Cluster 3 in the vicinity of the field reversal. The black and green arrows show the trajectories of Cluster 1 and Cluster 3 relative to the diffusion region. The blue lines show the magnetic field structure, including the expected quadrupole out-of-plane structure. The red arrows show the morphology of the Hall electric field. In the bottom half of the panel, qualitative time series variation of B_y and E_x are shown on the basis of the trajectory of the spacecraft relative to the structure. It is important to bear in mind that this cartoon does not interpret any time variations in the reconnection process that may be occurring, for example, changes in reconnection rate and the tailward ejection of the island.

flows has been observed in simulations and represents the direct action of the reconnection electric field on the ion population in the ion diffusion region. It is possible that such flows may also represent lateral motion of the magnetotail relative to the spacecraft or be part of the reconnection jet in an inherently three-dimensional structure. This effect needs to be investigated in future studies, in particular, by comparing these and similar data with the output of three-dimensional Hall and kinetic simulations.

[46] Both spacecraft begin in the upper left quadrant of the reconnection region. Cluster 3 then moves to the lower left quadrant, and Cluster 1 moves into the Hall region. Next, both spacecraft cross simultaneously to the tailward side of the reconnection site; we may conclude that the diffusion region itself passes between the spacecraft and was nested inside the tetrahedron. Figures 5 and 8 summarize the observed Hall effect fields. Cluster 1 then drifted close to the neutral sheet and observed a negligible Hall electric field before moving to the southern hemisphere. When Cluster 1 and Cluster 3 were on opposite sides of the current sheet, they observed mirror image Hall structure in both the electric and magnetic field. Asymmetry in the reconnection electric field (and thus the flow) is explained in part by the earthward motion of the X line, but cannot completely account for the observations; together with the asymmetry of other observations, this suggests temporal changes in the reconnection rate. We note in Figure 2 that the density and temperature observed by the two spacecraft do not vary significantly at the point of the flow and field reversal. Preliminary analysis shows that this is consistent with simulation results if, as is the case, the spacecraft moves parallel to the X-Y plane in the diffusion region (not shown).

[47] Shortly before the diffusion region encounter, Cluster 3, close to the current sheet, observed an extremely well defined flux rope. Theory, previous observations, and simulations all suggest that such loop-like structures ought to be a common phenomenon associated with the reconnection process, and given its close proximity to the flow reversal, we conclude that the two events are linked. This is somewhat similar to the observation of an island entrained in a magnetopause reconnection jet [*Retinò et al.*, 2006]. A second tailward-moving island was observed entrained in the tailward flow burst at 09:50 UT. This island was larger and observed by all the spacecraft. We do not describe it as a flux rope because there is no enhancement of the core magnetic field, and we do not observe any enhancement in the electric field.

[48] The earthward-moving flux rope observed at 09:42:48 by Cluster 3 is notable for the following two reasons: First, there was a significant enhancement of the core magnetic field. The guide field in the lobe, which is usually cited as the cause of the core enhancement, was negligible. However, the ambient B_y at the time of the flux rope encounter was approximately -10 nT, because of the Hall field associated with the diffusion region. It is currently unclear as to whether the flux rope core field can arise as a result of enhancement of the Hall field, particularly since the Hall field at the current sheet (and the presumed center of the flux rope) is zero, and more detailed comparisons with simulations are required. Second, electric fields of the order of 100 mV m^{-1} were observed in the center of the flux rope. The existence of the electric field structure as observed has not, as far as we are aware, been investigated theoretically or by simulations. Recent publications have reached different conclusions concerning the importance of islands in the production of energetic particles [*Drake et al.*, 2006a; *Pritchett*, 2006]; this new experimental information will have to be accounted for in future theoretical developments. A separate investigation has shown that this may not be a unique observation; electric fields of 60–80 mV m^{-1}, but with different structure, have been seen inside another small-scale flux rope [A. Retinò et al., private communication]. Further work establishing the statistics of electric fields inside flux ropes and comparing this data with simulations is underway.

[49] **Acknowledgment.** This work was supported by NASA grants NNG05GL27G and NNG05GE30G.

[50] Wolfgang Baumjohann thanks the reviewers for their assistance in evaluating this paper.

References

Arzner, K., and M. Scholer (2001), Kinetic structure of the post plasmoid plasma sheet during magnetic reconnection, *J. Geophys. Res.*, *106*, 3827–3844.

Asano, Y., T. Mukai, M. Hoshino, Y. Saito, H. Hayakawa, and T. Nagai (2004), Current sheet structure around the near-Earth neutral line observed by Geotail, *J. Geophys. Res.*, *109*, A02212, doi:10.1029/2003JA010114.

Balogh, A., et al. (2001), The Cluster magnetic field investigation: Overview of inflight performance and initial results, *Ann. Geophys.*, *19*, 1207–1217.

Birn, J., et al. (2001), Geospace Environmental Modeling (GEM) magnetic reconnection challenge, *J. Geophys. Res.*, *106*, 3715–3719.

Borg, A. L., M. Øieroset, T. Phan, F. S. Mozer, A. Pedersen, C. Mouikis, J. P. McFadden, C. Twitty, A. Balogh, and H. Rème (2005), Cluster encounter of a magnetic reconnection diffusion region in the near-Earth magnetotail on September 19, 2003, *Geophys. Res. Lett.*, *32*, L19105, doi:10.1029/2005GL023794.

Cattell, C. A., et al. (2005), Cluster observations of electron holes in association with magnetotail reconnection and comparison to simulations, *J. Geophys. Res.*, *110*, A01211, doi:10.1029/2004JA010519.

Daughton, W., J. D. Scudder, and H. Karimabadi (2006), Fully kinetic simulations of undriven magnetic reconnection with open boundary conditions, *Phys. Plasmas*, *13*, 072101.

Drake, J. F., M. A. Shay, W. Thongthai, and M. Swisdak (2005), Production of energetic electrons during magnetic reconnection, *Phys. Res. Lett.*, *94*, 095001.

Drake, J. F., M. Swisdak, H. Che, and M. A. Shay (2006a), Electron acceleration from contracting magnetic islands during reconnection, *Nature*, *443*, 553–556.

Drake, J. F., M. Swisdak, K. M. Schoeffler, B. N. Rogers, and S. Kobayashi (2006b), Formation of secondary islands during magnetic reconnection, *Geophys. Res. Lett.*, *33*, L13105, doi:10.1029/2006GL025957.

Dungey, J. W. (1961), Interplanetary magnetic field and the auroral zones, *Phys. Rev. Lett.*, *6*, 47–48.

Dunlop, M. W., D. J. Southwood, K.-H. Glassmeier, and F. M. Neubauer (1988), Analysis of multipoint magnetometer data, *Adv. Space Res.*, *8*, (9)273–(9)277.

Dunlop, M. W., A. Balogh, K.-H. Glassmeier, and P. Robert (2002), Four-point Cluster application of magnetic field analysis tools: The curlometer, *J. Geophys. Res.*, *107*(A11), 1384, doi:10.1029/2001JA005088.

Eastwood, J. P., A. Balogh, M. W. Dunlop, and C. W. Smith (2002), Cluster observations of the heliospheric current sheet and an associated magnetic flux rope and comparisons with ACE, *J. Geophys. Res.*, *107*(A11), 1365, doi:10.1029/2001JA009158.

Eastwood, J. P., D. G. Sibeck, J. A. Slavin, M. L. Goldstein, B. Lavraud, M. Sitnov, S. Imber, A. Balogh, E. A. Lucek, and I. Dandouras (2005), Observations of multiple X-line structure in the Earth's magnetotail current sheet: A Cluster case study, *Geophys. Res. Lett.*, *32*, L11105, doi:10.1029/2005GL022509.

Eastwood, J. P., D. G. Sibeck, J. A. Slavin, B. Lavraud, E. A. Lucek, A. Balogh, and I. Dandouras (2006), Observations of flux ropes and X-lines in the near earth magnetotail, in *Proc. Cluster and DoubleStar Symposium SP 598*, edited by K. Fletcher, ESA ESTEC, Noordwijk.

Elphic, R. C., C. A. Cattell, K. Takahashi, S. J. Bame, and C. T. Russell (1986), ISEE-1 and 2 observations of magnetic flux ropes in the magnetotail: FTE's in the plasma sheet?, *Geophys. Res. Lett.*, *13*, 648–651.

Escoubet, C. P., M. Fehringer, and M. L. Goldstein (2001), The Cluster mission, *Ann. Geophys.*, *19*, 1197–1200.

Fruit, G., P. Louarn, E. Budnik, J. A. Sauvaud, C. Jacquey, D. Le Quéau, H. Reme, E. A. Lucek, A. Balogh, and N. Cornilleau-Werhlin (2004), On the propagation of low-frequency fluctuations in the plasma sheet: 2. Characterization of the MHD eigenmodes and physical implications, *J. Geophys. Res.*, *109*, A03217, doi:10.1029/2003JA010229.

Fujimoto, M., M. S. Nakamura, I. Shinohara, T. Nagai, T. Mukai, Y. Saito, T. Yamamoto, and S. Kokubun (1997), Observations of earthward streaming electrons at the trailing boundary of a plasmoid, *Geophys. Res. Lett.*, *24*, 2893–2896.

Gustafsson, G., et al. (2001), First results of electric field and density observations by Cluster EFW based on initial months of operation, *Ann. Geophys.*, *19*, 1219–1240.

Henderson, P. D., C. J. Owen, L. V. Alexeev, J. A. Slavin, A. N. Fazakerley, E. A. Lucek, and H. Rème (2006), Cluster observations of flux rope structures in the near-tail, *Ann. Geophys.*, *24*, 651–666.

Hesse, M., J. Birn, D. Baker, and J. A. Slavin (1996), MHD simulations of the transition of magnetic reconnection from closed to open field lines, *J. Geophys. Res.*, *101*, 10,805–10,816.

Hesse, M., K. Schindler, J. Birn, and M. Kuznetsova (1999), The diffusion region in collisionless magnetic reconnection, *Phys. Plasmas*, *6*, 1781–1795.

Hesse, M., J. Birn, and M. Kuznetsova (2001), Collisionless magnetic reconnection: Electron processes and transport modeling, *J. Geophys. Res.*, *106*, 3721–3735.

Lin, R. P., et al. (2003), RHESSI observations of particle acceleration and energy release in an intense solar gamma-ray line flare, *Astrophys. J.*, *595*, L69–L76.

Louarn, P., G. Fruit, E. Budnik, J. A. Sauvaud, C. Jacquey, D. Le Quéau, H. Reme, E. A. Lucek, and A. Balogh (2004), On the propagation of low-frequency fluctuations in the plasma sheet: 1. Cluster observations and magnetohydrodynamic analysis, *J. Geophys. Res.*, *109*, A03216, doi:10.1029/2003JA010228.

Lui, A. T., Y. Zheng, Y. Zhang, S. Livi, H. Reme, M. W. Dunlop, G. Gustafsson, S. B. Mende, C. Mouikis, and L. M. Kistler (2006), Cluster observations of plasma flow reversal in the magnetotail during a substorm, *Ann. Geophys.*, *24*, 2005–2013.

Mozer, F. S., S. D. Bale, and T. D. Phan (2002), Evidence of diffusion regions at a subsolar magnetopause crossing, *Phys. Rev. Lett.*, *89*, 015002.

Nagai, T., I. Shinohara, M. Fujimoto, M. Hoshino, Y. Saito, S. Machida, and T. Mukai (2001), Geotail observations of the Hall current system: Evidence of magnetic reconnection in the magnetotail, *J. Geophys. Res.*, *106*, 25,929–25,949.

Nakamura, R., W. Baumjohann, Y. Asano, A. Runov, A. Balogh, C. J. Owen, A. N. Fazakerley, M. Fujimoto, B. Klecker, and H. Reme (2006), Dynamics of thin current sheets associated with magnetotail reconnection, *J. Geophys. Res.*, *111*, A11206, doi:10.1029/2006JA011706.

Ohtani, S., M. A. Shay, and T. Mukai (2004), Temporal structure of the fast convective flow in the plasma sheet: Comparison between observations and two-fluid simulations, *J. Geophys. Res.*, *109*, A03210, doi:10.1029/2003JA010002.

Øieroset, M., T. D. Phan, M. Fujimoto, R. P. Lin, and R. P. Lepping (2001), In situ detection of collisionless reconnection in the Earth's magnetotail, *Nature*, *412*, 414–417.

Pritchett, P. L. (2001a), Collisionless magnetic reconnection in a three-dimensional open system, *J. Geophys. Res.*, *106*, 25,961–25,977.

Pritchett, P. L. (2001b), Geospace Environment Modeling magnetic reconnection challenge: Simulations with a full particle electromagnetic code, *J. Geophys. Res.*, *106*, 3783–3798.

Pritchett, P. L. (2005a), Externally driven magnetic reconnection in the presence of a normal magnetic field, *J. Geophys. Res.*, *110*, A05209, doi:10.1029/2004JA010948.

Pritchett, P. L. (2005b), Onset and saturation of guide-field magnetic reconnection, *Phys. Plasmas*, *12*, 062301.

Pritchett, P. L. (2006), Relativistic electron production during driven magnetic reconnection, *Geophys. Res. Lett.*, *33*, L13104, doi:10.1029/2005GL025267.

Rème, H., et al. (2001), First multispacecraft ion measurements in and near the Earth's magnetosphere with the identical Cluster ion spectrometry (CIS) experiment, *Ann. Geophys.*, *19*, 1303–1354.

Retinò, A., et al. (2006), Structure of the separatrix region close to a magnetic reconnection X-line: Cluster observations, *Geophys. Res. Lett.*, *33*, L06101, doi:10.1029/2005GL024650.

Runov, A., et al. (2003), Current sheet structure near magnetic X-line observed by Cluster, *Geophys. Res. Lett.*, *30*(11), 1579, doi:10.1029/2002GL016730.

Schindler, K. (1974), A theory of the substorm mechanism, *J. Geophys. Res.*, *79*, 2803–2810.

Schwartz, S. J. (1998), Shock and Discontinuity Normals, Mach Numbers and Related Parameters, in *Analysis methods for multi-spacecraft data*, edited by G. Paschmann and P. W. Daly, pp. 249–270, International Space Science Institute, Bern.

Shay, M. A., J. F. Drake, R. E. Denton, and D. Biskamp (1998), Structure of the dissipation region during collisionless magnetic reconnection, *J. Geophys. Res.*, *103*, 9165–9176.

Shay, M. A., J. F. Drake, B. N. Rogers, and R. E. Denton (2001), Alfvenic collisionless magnetic reconnection and the Hall term, *J. Geophys. Res.*, *106*, 3759–3772.

Shay, M. A., J. F. Drake, M. Swisdak, and B. N. Rogers (2004), The scaling of embedded collisionless reconnection, *Phys. Plasmas*, *11*, 2199–2213.

Sitnov, M., A. S. Sharma, P. N. Guzdar, and P. H. Yoon (2002), Reconnection onset in the tail of Earth's magnetosphere, *J. Geophys. Res.*, *107*(A9), 1256, doi:10.1029/2001JA009148.

Slavin, J. A., R. P. Lepping, J. Gjerloev, D. H. Fairfield, M. Hesse, C. J. Owen, M. B. Moldwin, T. Nagai, A. Ieda, and T. Mukai (2003a), Geotail observations of magnetic flux ropes in the plasma sheet, *J. Geophys. Res.*, *108*(A1), 1015, doi:10.1029/2002JA009557.

Slavin, J. A., et al. (2003b), Cluster current density measurements within a magnetic flux rope in the plasma sheet, *Geophys. Res. Lett.*, *30*(7), 1362, doi:10.1029/2002GL016411.

Slavin, J. A., E. Tanskanen, M. Hesse, C. J. Owen, M. W. Dunlop, S. Imber, E. A. Lucek, A. Balogh, and K.-H. Glassmeier (2005), Cluster observations of traveling compression regions in the near-tail, *J. Geophys. Res.*, *110*, A06207, doi:10.1029/2004JA010878.

Sonnerup, B. U. Ö. (1979), Magnetic Field Reconnection, in *Solar System Plasma Physics Volume III*, edited by L. T. Lanzerotti, C. F. Kennel, and E. N. Parker, pp. 47–108, Elsevier, New York.

Sonnerup, B. U. Ö., and M. Scheible (1998), Minimum and Maximum Variance Analysis, in *Analysis Methods for Multi-Spacecraft Data*, edited by G. Paschmann and P. W. Daly, pp. 185–220, International Space Science Institute, Bern.

Ueno, G., S. Machida, T. Mukai, Y. Saito, and A. Nishida (1999), Distribution of X-type magnetic neutral lines in the magnetotail with Geotail observations, *Geophys. Res. Lett.*, *26*, 3341–3344.

Vaivads, A., Y. Khotyaintsev, M. André, A. Retinò, S. Buchert, B. N. Rogers, P. Décréau, G. Paschmann, and T. D. Phan (2004), Structure of the magnetic reconnection diffusion region from four-spacecraft observations, *Phys. Res. Lett.*, *93*, 105001.

Vasyliunas, V. M. (1975), Theoretical models of magnetic field line merging, 1, *Rev. Geophys.*, *13*, 303–336.

Volwerk, M., et al. (2004), Compressional waves in the Earth's neutral sheet, *Ann. Geophys.*, *22*, 303–315.

Wygant, J. R., et al. (2005), Cluster observations of an intense normal component of the electric field at a thin reconnecting current sheet in the tail and its role in the shock-like acceleration of the ion fluid into the separatrix region, *J. Geophys. Res.*, *110*, A09206, doi:10.1029/2004JA010708.

Xiao, C. J., et al. (2006), In situ evidence for the structure of the magnetic null in a 3D reconnection event in the Earth's magnetotail, *Nat. Phys.*, *2*, 478–483.

A. Balogh and E. A. Lucek, Space and Atmospheric Physics, The Blackett Laboratory, Imperial College, London, London, UK.

I. Dandouras, CESR - CNRS/UPS, Toulouse, France.

J. P. Eastwood, F. S. Mozer, and T.-D. Phan, Space Sciences Laboratory, University of California Berkeley, 7 Gauss Way, Berkeley, CA 94720, USA. (eastwood@ssl.berkeley.edu)

M. Fujimoto, Solar-Terrestrial Physics Group, Institute of Space and Astronautical Science, Sagamihara, Kanagawa, Japan.

M. Hesse, Geospace Physics Branch, Laboratory for Solar and Space Physics, NASA Goddard Space Flight Center, Greenbelt, MD, USA.

A. Retinò, Swedish Institute of Space Physics, Uppsala, Sweden.

M. A. Shay, Department of Physics and Astronomy, University of Delaware, Newark, DE, USA.